frontiers | Frontiers in Materials

TYPE Original Research
PUBLISHED 20 December 2022
DOI 10.3389/fmats.2022.979151

OPEN ACCESS

EDITED BY
Giuseppe Puglisi,
Politecnico di Bari, Italy

REVIEWED BY
Behrad Koohbor,
Rowan University, United States
Giuseppe Zurlo,
University of Galway, Ireland

*CORRESPONDENCE
Maximilian Jentzsch,
maximilian.jentzsch@biologie.uni-freiburg.de

SPECIALTY SECTION
This article was submitted to Mechanics of Materials, a section of the journal Frontiers in Materials

RECEIVED 11 August 2022
ACCEPTED 07 December 2022
PUBLISHED 20 December 2022

CITATION
Jentzsch M, Badstöber M-C, Umlas F and Speck T (2022), Damage protection in fruits: Comparative analysis of the functional morphology of the fruit peels of five *Citrus* species *via* quasi-static compression tests.
Front. Mater. 9:979151.
doi: 10.3389/fmats.2022.979151

Damage protection in fruits: Comparative analysis of the functional morphology of the fruit peels of five *Citrus* species *via* quasi-static compression tests

Maximilian Jentzsch [1,2]*, Marie-Christin Badstöber [1], Franziska Umlas [1] and Thomas Speck [1,2,3,4]

[1]Plant Biomechanics Group, Faculty of Biology, University of Freiburg, Freiburg, Germany, [2]Cluster of Excellence livMatS @ FIT, Freiburg, Germany, [3]Freiburg Materials Research Center (FMF), Freiburg, Germany, [4]Freiburg Center for Interactive Materials and Bioinspired Technologies (FIT), Freiburg, Germany

Due to their special peel tissue, comprising a dense flavedo (exocarp), a less dense albedo (mesocarp), and a thin endocarp, most citrus fruits can withstand the drop from a tree or high shrub (relatively) undamaged. While most citrus fruit peels share this basic morphological setup, they differ in various structural and mechanical properties. This study analyzes how various properties in citrus peels of the pomelo, citron, lemon, grapefruit, and orange affect their compression behavior. We compare the structural and biomechanical properties (e.g., density, stress, Young's modulus, Poisson's ratio) of these peels and analyze which properties they share. Therefore, the peels were quasi-statically compressed to 50% compression and analyzed with manual and digital image correlation methods. Furthermore, local deformations were visualized, illustrating the inhomogeneous local strain patterns of the peels. The lateral strain of the peels was characterized by strain ratios and the Poisson's ratio, which were close to zero or slightly negative for nearly all tested peels. Our findings prove that—despite significant differences in stress, magnitude, distribution, and thickness - the tested peels share a low Poisson's ratio meaning that the general peel structures of citrus species offer a promising inspiration for the development of energy dissipating cellular structure that can be used for damage protection.

KEYWORDS

damage protection, *Citrus spp.*, fruit peel, poisson's ratio, quasi-static compression, biomechanics, digital image correlation

1 Introduction

Citrus fruits widely vary, mainly with differences in color, taste and size, however despite this variability all citrus can be categorized into three distinct basal species: pomelo, citron, and mandarin (Moore 2001; Klock et al., 2007; Ladaniya 2008; Gentile et al., 2020). Besides these morphological and physiological characteristics, the anatomical structure of citrus peels causes some preferable mechanical properties such as a high energy dissipation (Seidel et al., 2010; Thielen et al., 2015; Yang et al., 2022). Even if the proportion and fine structure of individual tissues of the fruit differ, the peel typically consists of an epidermis, a parenchymatous flavedo (exocarp), a thicker, less dense albedo (mesocarp) and a thin endocarp (Ford 1942; Scott and Baker 1947; Jentzsch et al., 2022). In this article, we use quasi-static compression tests to investigate the compression behavior of the peel of pomelo (*C. maxima*), citron (*C. medica*), lemon (*C.* x *limon*), grapefruit (*C.* x *paradisi*) and orange (*C.* x *sinensis*) to better understand damage protection properties. The aim is to obtain an overview of the compression behavior and in particular, the lateral compression of these citrus fruit peels.

The Poisson's ratio is an essential quantity when it comes to characterizing the compression behavior of materials in an elastic range. It generally describes the negative ratio of axial and lateral compression (Evans 1991). For isotropic elastic materials the numerical limits of the Poisson's ratios are set by −1 and 0.5 (Lakes 1987; Evans 1991). For anisotropic elastic materials, however, values highly depend on the orientation of the material and can assume arbitrarily large or small values under specific conditions (Ting and Chen 2005). While a high Poisson's ratio is related to a strong lateral enlargement of the material under axial compression, no lateral deformation occurs in a material with a Poisson's ratio of zero (Lakes 1987). In contrast, a material loaded by axial pressure that also contracts in lateral dimension results in a negative Poisson's ratio (Alderson 1999; Ashjari 2017). These materials are also known as auxetic materials (Evans 1991). While rubbers and soft biological tissues typically show a Poisson's ratio of approximately 0.5 (Lakes 1987; Evans 1991), steel and other metals typically show a ratio of about 0.3 (Lakes 1987; Evans 1991). Poisson's ratio of polymer foams typically fall in a range of 0.1–0.4 (Lakes 1987) while cork is characterized by a Poisson's ratio of close to 0 (Lakes 1987).

A negative Poisson's ratio is rarely observed in natural materials and primarily occurs as a structural property due to a special material configuration (metamaterials), such as in special technical man-made open-cell foams (Ashjari 2017). Currently, there are a variety of structural demonstrators and systems that exhibit auxetic properties (Ashjari 2017; Ren et al., 2018). Although there is a steady increase in new designs and developments of e.g. polymeric foams with corresponding properties (Koumlis and Lamberson 2019; Youssef et al., 2022), it is still rare to find a commercial, cost-effective, and easy-to-manufacture auxetic product suitable for large-scale fabrication. Nonetheless, material systems with very low or even negative lateral compression offer high potential for applications in impact protection and energy absorption in areas ranging from aerospace applications (Alderson and Alderson 2007) to packaging (Seidel et al., 2010; Li et al., 2019) to protective equipment (Allen et al., 2015; Speck et al., 2018). This is because the material is compacted in a loading case, it adapts to the impact, making it more difficult to penetrate the material and dissipates more energy compared to conventional material systems with a positive Poisson's ratio (Alderson 1999).

Material systems that adapt to a stimulus and change their state are called classical responsive systems (Walther 2020). Dissipative systems, on the other hand, autonomously return to their original state as soon as the stimulus changes or ends, e.g. when the compression of a material ends and the material returns to its initial state under elastic deformation or when relaxation occurs due to viscoelastic behavior. This is even more promising because they do not need any antagonistic stimulus and can directly respond to another stimulus, which is in contrast to a classical responsive system. These dissipative systems illustrate a transformation from classical responsive systems, in terms of material properties, and is the first step towards adaptive and interactive systems. This step forward is also a step towards so-called living materials systems or materials with life-like behavior (Walther 2020). Towards that end, living nature offers inspiration for apparent auxetic structures, which are characterized, for example, by excellent energy dissipation properties. Examples include the peel of pomelo, which highly dissipates energy under (quasi-) static as well as under dynamic loading (Fischer et al., 2010; Seidel et al., 2010; Thielen et al., 2015; Jentzsch et al., 2022; Yang et al., 2022). In addition, various citrus fruits peels have also been described as biological functionally graded materials (FGM) (Jentzsch et al., 2022). Wang et al. (2018) calculated a Poisson's ratio of 0.08–0.11 ± 0.02 for the pomelo peel, at compression levels of up to 50%. Yang et al. (2022) investigated the Poisson's ratios of different pomelo species using compression tests of up to 20% strain. They divided the fruit peel into three regions: outer (close to the epidermis), middle (albedo), and inner (close to the pulp). The Poisson's ratio of the pomelo peel for the middle region is reported to be close to zero with a range of −0.032 to 0.035. The inner region has a range of 0.01–0.071 and the outer region a range of 0.239–0.346. These Poisson's ratios indicate a promising compression behavior followed by a very low and partially negative lateral compression for the middle and inner region. Consequently, these studies indicate that the peel of the pomelo has high potential to be a biological source of inspiration for technical material systems and damage protection applications. Taken together, this suggests that other species of *Citrus* may also show low or even negative Poisson's ratios due to their similar anatomy what was the starting point for the present study.

TABLE 1 Overview of species used and varieties of *Citrus* spp. for quasi-static compression tests.

Species	Variety	Trivial name	Number of fruits	Origin
Citrus maxima	honey pomelo red	Pomelo	10	China
Citrus medica	Nasone	Citron	5	Italy
Citrus x *limon*	Verna	Lemon	9	Spain
Citrus x *paradisi*	star ruby	Grapefruit	6	Spain
Citrus x *sinensis*	lane late	Orange	5	Spain

2 Materials and methods

2.1 Plant material

For this study, untreated fruits were purchased from local suppliers and stored (for 1–5 days) at ambient conditions until further examination. Only fruits without any external damage were selected. The number and country of origin of the respective fruits are shown in Table 1. For comprehensibility, the species are listed by their trivial names as shown in Table 1.

2.2 Sample preparation

The fruits were cut cross-sectionally in the equatorial region. To measure the relative proportion of the peel, images of the cross-sections of each fruit were taken and analyzed with the software Fiji/ImageJ (Version 1.52a). To determine the thickness of the flavedo, thin sections (3–5 µm) were dissected from the cross-sections using a rotary microtome (CUT 5062, SLEE medical GmbH, Nieder-Olm, Germany) and then analyzed using a light microscope (BX61, Olympus, Hamburg, Germany). In addition, to calculate the density of the peel, cylindrical samples (diameter: 17.75 ± 0.02 mm) were dissected. They were weighed (ABT 120-5DNM, KERN, Balingen, Germany; accuracy: ±0.1 mg) and measured using a digital caliper (Mitutoyo 500-161U, UK; accuracy: ±0.03 mm). For mechanical characterization, cubic samples were cut from the equatorial section (size 17 × 17 mm, with a specific species dependent sample thickness). To do so, the samples were first separated from the pulp with a razor blade. To prevent any dehydration, each sample was excised immediately before it was tested. In addition to the respective peel samples, cubic samples of an open-cell polyurethane foam (RG 35/50, Nanoform Airbag Sports GmbH, Spenge, Germany) were tested in order to create a technical comparison (comparatively sized to the fruit peel samples: 17 × 17 × 6.5 mm and 17 × 17 × 20 mm). To analyze the compression behavior, two different methods were used. One part of the samples was analyzed manually using the software Fiji/ImageJ (version 1.52a) (MIC) (inspired by Widdle et al., 2008), while another part of the samples was studied using the digital image correlation software GOM-Correlate (version 2019 Hotfix 7, Rev. 128764) (DIC). Depending on the analysis method, different patterns were applied to the samples (Figure 1). To calculate the strain, either the dot distance or the tracking points were measured, before and after testing. For MIC, an equidistant dot pattern was applied using a stencil (the dot centers were spaced 4 mm (citron) or 3 mm (pomelo, lemon, grapefruit, orange, and PU foam)) (Figure 1A). For the digital image correlation, on the other hand, a stochastic dot pattern was sprayed onto the samples (Figure 1B).

2.3 Mechanical testing

Regardless of the analysis method, all specimens were mechanically tested with the same method. The sample size for each species per analysis method are shown in Table 2. Generally, the tests were performed on a universal testing machine with a load cell of 1 kN (Inspekt table 5 kN, Hegewald & Peschke, Nossen, Germany). For the quasi-static compression tests, compression plates were clamped in the testing machine. Before each measurement, the distance between the two compression plates was re-tared via the inverse position. Thereafter, the test specimen were centered on the lower plate while the upper compression plate was moving at a speed of 10 mm/min onto the specimen until a pre-load of 0.1 N was reached. Reaching the pre-load initiated the beginning of the compression measurement and corresponded to a compression of the specimen of 0%. In a loop, the specimen was compressed by 5% at a test speed of 5 mm/min and the position of the compression plate was held for 100 s in a subsequent relaxation phase. The test ended with a relaxation phase after an axial compression of 50% was reached. During the test, the specimen was recorded with a camera (Panasonic Lumix DMC-FZ1000, Panasonic Deutschland, Wiesbaden, Germany) at a frequency of 1 fps. The camera was placed at a distance of 25 cm perpendicular to the patterned sample area. The recording started automatically and stopped manually after each experiment. Due to variability in peel thickness, testing time for the mechanical compression differed for each specimen because the test speed remained constant (5 mm/min). The

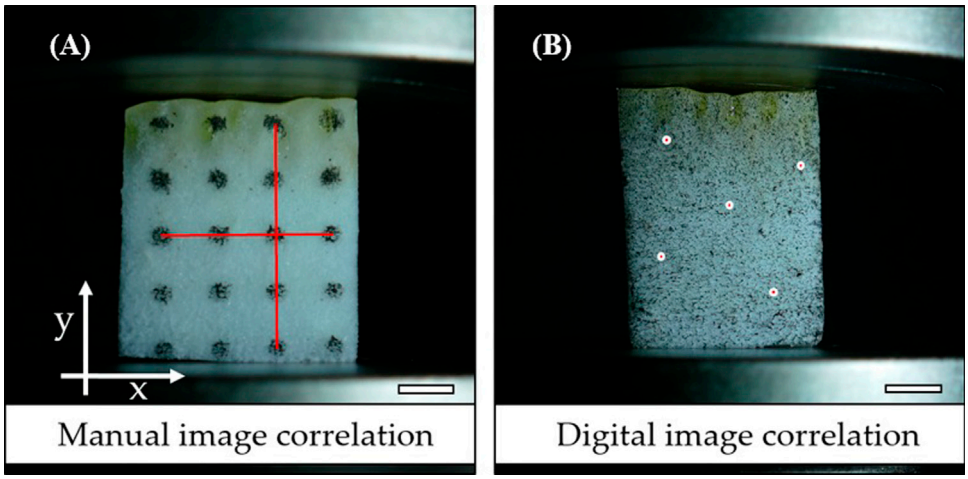

FIGURE 1
Characteristic samples of a citron peel (*C. medica*) with **(A)** an equidistant dot pattern and red lines for manual image correlation (MIC) and **(B)** a stochastic pattern for digital image correlation (DIC). Scale bar equals 5 mm.

TABLE 2 Sample sizes of the species used of *Citrus* spp. [pomelo (*C. maxima*), citron (*C. medica*), lemon (*C.* x *limon*), grapefruit (*C.* x *paradisi*), orange (*C.* x *sinensis*)] for quasi-static compression tests with digital image correlation (DIC) or manual image correlation (MIC).

Species	Sample size DIC-method	Sample size MIC-method
C. maxima	14	15
C. medica	11	12
C. x *limon*	13	12
C. x *paradisi*	12	12
C. x *sinensis*	12	12

images of the specimens at each compression level were selected manually. The first image of the specimen (at 0% compression) was made in an uncompressed state before the test started to achieve the pre-load.

2.3.1 Manual image correlation (MIC)

Based on the applied dot pattern (Figure 1A), the dot-distance on each peel sample was measured using the software ImageJ/Fiji (accuracy: 0.01 mm). The outer two middle points in vertical and horizontal directions were each connected with a line (red lines, Figure 1A). To determine the strain (ε_x, ε_y) of the samples, the change in length of the lines in lateral (Δd) and axial (Δl) direction was calculated and divided by the initial length of the straight line (d_0, l_0). The negative ratio of strain is also called Poisson's ratio (υ) and quantifies the strain in the elastic range. If there was no clear elastic range, the Poisson's ratios were calculated at a low axial strain of 10%. To also characterize the compression behavior of the peel for higher strain levels (20%–50%) were the elastic range was left, the strain ratios of the specimen were calculated for each strain level by the same formula as used to assess the Poisson's ratio.

$$\upsilon = -\frac{\varepsilon_x}{\varepsilon_y} = -\frac{\Delta d/d_0}{\Delta l/l_0} \quad (1)$$

2.3.2 Digital image correlation (DIC)

For this analysis method, a stochastic point pattern was sprayed on the samples (Figure 1B). For each of the compression levels, from 0% to 10%, one image was selected and imported manually into the program GOM-Correlate 2019. The image without compression (strain-level 0%) was set as a reference stage. First, the facet settings were defined. The settings which best suited the task were: facet size: 24 pixels, facet distance: 16 pixels, calculation-method: more points and facet-matching: against reference level. Pre-evaluated experiments showed that these settings cover the range for reasonable surface detection. The sample surface was then selected using polygonal facets. To track the deformation,

five tracking points were assigned to the sample and applied to all compression levels. If the software lost a facet at a compression level, it was not re-added at subsequent compression levels. By selecting the five points, continuous tracking throughout the various strain-levels was ensured (dots, Figure 1B). The dots were selected randomly throughout the whole peel. Finally, for each point, at each of the compression levels, a strain in axial (ε_y) and lateral (ε_x) direction could be read. These five points were used to calculate a compression in and perpendicular to the force direction for each strain level. The Poisson's ratio of the specimen was determined by the negative ratio of the strain in both directions. Additionally, the strain in the lateral direction was also visualized via the software GOM Correlate.

2.4 Statistical analyses

Statistical testing was performed with the software R (version 4.0.0) and the user interface R-Studio (version 1.2.5042) (R Core Team 2019). To select the statistical test method we first divided the data into: parametric and non-parametric and then further divided the data by group size into ≤2 or >2. In addition, we took into consideration whether the groups were dependent or independent. Using a Shapiro test, the groups were tested for normal distribution. For normally distributed data, a mean and standard deviation (sd) was given, if a group of a data set was not normally distributed, median and interquartile range (IQR) were given for the whole data set. The homogeneity of variances was checked with a Levene test.

For parametric data that had a group size ≤2 and had homogeneous variances, a *t*-test (independent data) or paired *t*-test (dependent data) was performed. For heterogeneous variances, a Welch test was performed. For parametric data that had a group size >2 and had homogeneous variances, an ANOVA was performed for independent data. For dependent data, repeated-measures ANOVA was performed, followed by a TukeyHSD test. For heterogeneous variances in the data, a Kruskal–Wallis test was performed. A Wilcoxon-Mann-Withney *t*-test was performed for non-parametric independent data with a group size ≤2. For non-parametric dependent data with a group size ≤2, a paired Wilcoxon test was performed. If the data set was >2 groups of non-parametric independent data, a Kruskal-Wallis test followed by a paired-Wilcoxon test was performed (with Holm correction). If the data sets were dependent on each other, a repeated measures Kruskal-Wallis test was applied. Significantly different data sets were considered to exist if the probability of error was <5% ($p < 0.05$). The level of statistical significance is indicated as: *: $0.01 \leq p < 0.05$ (significant); **: $0.001 \leq p < 0.01$ (high significant); ***: $p < 0.001$ (highest significant).

3 Results

3.1 Morphology

The five species optically differ in size and pulp color (Figure 2). We analyzed the fruits for significant differences in their peel proportion, peel thickness, and peel density (Table 3).

In comparing the relative peel proportions, it becomes apparent that almost all of the fruits differ significantly ($p < 0.001$) from each other in their peel proportions (Table 3). The only exceptions are between grapefruit (27.77%) and orange (26.04%) and between pomelo (46.93%) and lemon (37.63%) for which no significant differences were found. These species are not significantly different from each other in their peel proportion ($p > 0.05$). Citron shows the highest peel proportion with 65.68% and grapefruit and orange show the lowest peel proportions with 27.77% and 26.04% respectively. The peel density is significantly different ($p < 0.001$) for all tested species, except lemon (784 kg/m^3) and orange (746 kg/m^3) ($p > 0.05$). The peel of lemon and orange have the highest density, whereas the peel of pomelo (354 kg/m^3) has the lowest. The sample thickness distribution is similar to the peel density distribution. The two thinnest peels, lemon (5.9 mm) and orange (6.2 mm), do not differ significantly from each other. The other fruits differ in their peel thickness significantly ($p < 0.001$). The largest peel thickness is measured for citron (18.5 mm).

3.2 Stress and force

The samples were quasi-statically compressed to 50% of their original height. Except for citron and pomelo, all specimens experienced significant different maximum forces and stresses ($p < 0.001$). Between citron and pomelo also a significant difference is found ($0.001 \leq p < 0.01$) (Table 4). To compress the fruits to 50%, the lemon required the highest median max. force of 326.10 N, whereas the pomelo required the lowest median max. Force with a value of 40.32 N. The samples of the PU foam showed no significant differences ($p > 0.05$) for both test heights (6.5 mm and 20 mm), neither for the max. force nor for the max. stress, which is why the samples were pooled. Compared to the natural specimens, the force values for the PU foam samples are significantly lower ($p < 0.001$) and required a max. force of 2.74 N (0.17 N) to achieve a compression of 50%. Citron (75.40 kPa) and pomelo (50.40 kPa) exhibit the largest Young's modulus compared to the other samples (Table 4). The orange peel has the lowest Young's modulus (19.85 kPa), it is significantly lower ($0.001 \leq p < 0.01$) than the Young's modulus of the pomelo peel and it is significantly lower ($p < 0.001$) than the Young's modulus of the other samples. Only when compared to grapefruit, does the orange not reveal a significant difference ($p > 0.05$). The

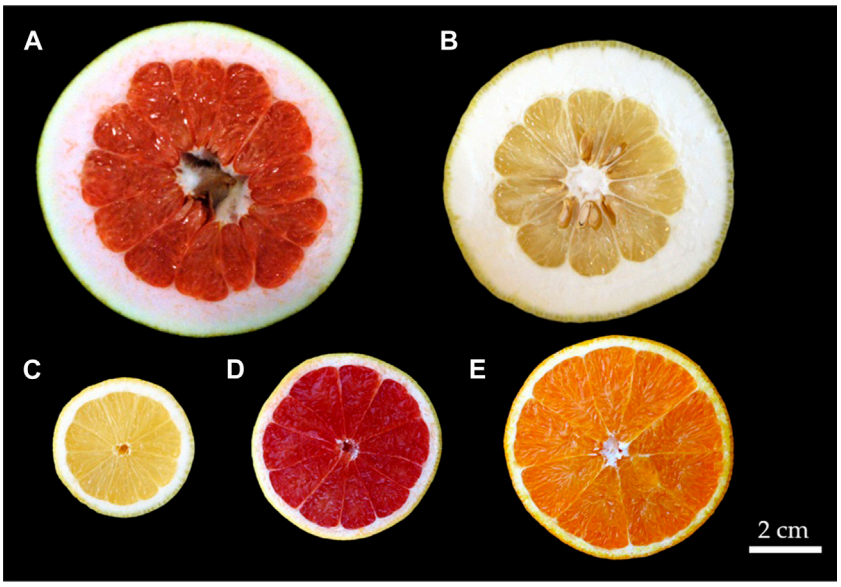

FIGURE 2
Equatorial cross-section of the fruits of **(A)** pomelo (*C. maxima*) **(B)** citron (*C. medica*) **(C)** lemon (*C.* x *limon*) **(D)** grapefruit (*C.* x *paradisi*), and **(E)** orange (*C.* x *sinensis*).

TABLE 3 Median data of the fruit and peel anatomy of *Citrus* spp. [pomelo (*C. maxima*), citron (*C. medica*), lemon (*C.* x *limon*), grapefruit (*C.* x *paradisi*), orange (*C.* x *sinensis*)].

Species	Peel proportion (%)	Peel density (kg/m^3)	Peel thickness (mm)
C. maxima	46.93 (13.66) (n = 10)	354 (59) (n = 30)	12.9 (4.2) (n = 30)
C. medica	65.68 (4.55) (n = 15)	532 (41) (n = 29)	18.5 (3.9) (n = 28)
C. x *limon*	37.63 (9.13) (n = 20)	784 (96) (n = 15)	5.9 (0.6) (n = 26)
C. x *paradisi*	27.77 (6.09) (n = 15)	613 (78) (n = 26)	8.4 (2.7) (n = 26)
C. x *sinensis*	26.04 (7.88) (n = 15)	746 (172) (n = 26)	6.2 (0.8) (n = 26)

TABLE 4 Median stress of the peel samples and applied force at a strain level of 50% compression; pomelo (*C. maxima*), citron (*C. medica*), lemon (*C.* x *limon*), grapefruit (*C.* x *paradisi*), orange (*C.* x *sinensis*). Median Young's Modulus is calculated up to a strain of 0.5% compression. PU foam (RG35/50) specimens with both sample heights (6.5 mm and 20 mm) were pooled for max. stress, applied force, and Young's Modulus.

Species	n		Max. stress (MPa)	Max. applied force (N)	Young's modulus (kPa)	Test duration (min)	
C. maxima	30		0.15 (0.13)	40.32 (35.62)	50.40 (44.05)	17.91 (0.31)	
C. medica	28		0.18 (0.04)	50.57 (14.97)	75.40 (43.62)	18.53 (0.40)	
C. x limon	26		1.14 (0.27)	326.10 (83.49)	36.40 (27.95)	17.31 (0.07)	
C. x paradisi	26		0.26 (0.11)	72.05 (29.55)	25.70 (19.80)	17.54 (0.24)	
C. x sinensis	26		0.51 (0.09)	147.97 (22.03)	19.85 (10.90)	17.33 (0.06)	
PU foam (RG35/50)	20	20	0.01 (0.00)	2.74 (0.17)	40.15 (34.80)	17.33 (0.01)	18.68 (0.03)

lemon's Young's modulus is significantly lower than the one of citron ($0.001 \leq p < 0.01$) and significantly higher ($p < 0.001$) than that of orange. The PU foam has an intermediate Young's modulus of 40.15 kPa, compared to the tested fruit peels. It differs significantly ($p < 0.001$) from pomelo, citron, and orange. The ranking of test duration is similar to the peel

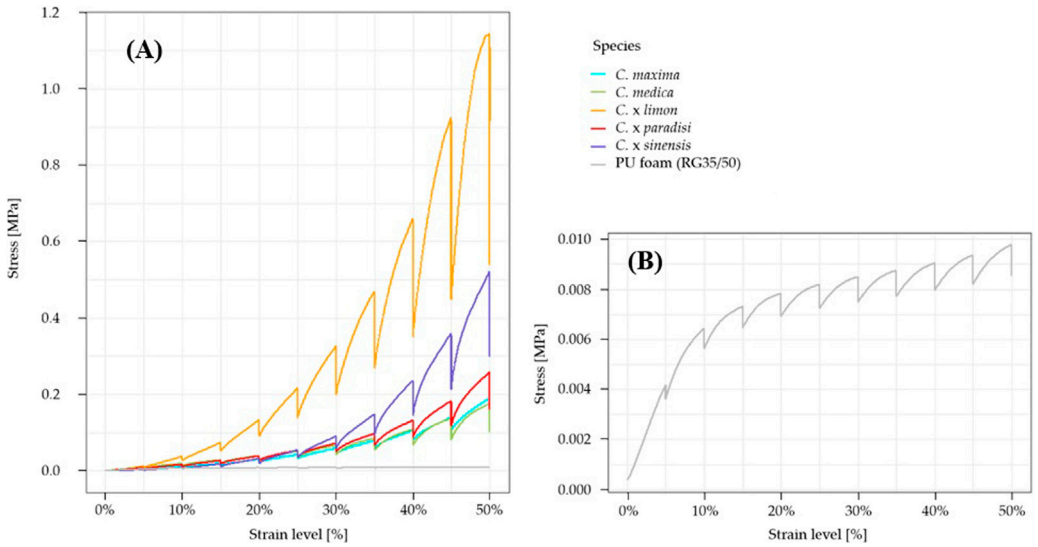

FIGURE 3
Characteristic stress-strain diagrams **(A)** for a specimen of each tested citrus species: pomelo (*C. maxima*), citron (*C. medica*), lemon (*C.* x *limon*), grapefruit (*C.* x *paradisi*), orange (*C.* x *sinensis*), and PU foam (RG 35/50) **(B)** Zoomed illustration of a characteristic stress-strain diagram of the PU foam (RG35/50).

thickness ranking, as the thickest peel requires the longest test duration. The test durations of the different citrus samples differ significantly from each other ($p < 0.001$), only lemon and orange show no significant difference between each other ($p > 0.05$). In addition, the test duration of the PU foams with a sample height of 6.5 mm is not significantly lower ($p > 0.05$) than the test duration of lemon and orange. Furthermore, the test duration of citron and the PU foam with a sample height of 20 mm is also not significantly lower ($p > 0.05$).

For all tested *Citrus* species, the characteristic stress-strain diagrams show a similar pattern (Figure 3). While the amount of stress differs, the stress increases during compression and decreases in the relaxation phase. With increasing compression, the stress decreases and increases during relaxation in a regular sequence. There is no clear elastic range visible in the stress-strain diagrams of *Citrus* spp. The Young's modulus was calculated by a linear regression up to a compression of 0.5% for each sample, to ensure that the elastic range was covered. The stress-strain diagrams are slightly concave with increasing strain level. For the tested *Citrus* species, the highest stresses and relaxations occurred in the stress-strain graphs of lemon. Regarding the stress-strain diagrams of the PU foam, the stresses are significantly lower ($p > 0.05$) compared to those of all *Citrus* spp. For PU foam, the stress decreases relatively constantly with increasing compression level in the relaxation phases (Figure 3B). The general stress-strain graphs of the PU foam differ from those of the citrus samples. While the stress of the citrus samples increases more steeply with increasing compression, the stress of the PU foam increases less steeply, indicating the PU foam reaches a plateau.

3.3 Strain ratio and lateral strain for higher strain levels

3.3.1 Manual image correlation (MIC)

Due to the fact that there is no clear elastic range in the stress-strain diagrams of *Citrus* spp. (Figure 3) we determined the Poisson's ratio at a low axial strain level of 10% and compared the Poisson's ratios for both methods (MIC and DIC). To describe the deformation behavior for higher strain levels (>10%) the strain ratios are calculated to compare the deformation during the whole compression test. The strain ratios for higher strain levels (>10%) are calculated the same way that the Poisson's ratio is calculated. The strain ratios of all tested *Citrus* species are close to zero or slightly negative, with exception of lemon for which the values range between 0.00 and 0.20 (Table 5). The strain ratio values of the pomelo decrease with an increasing compression level (Supplementary Figure S1). Regarding the strain levels of the pomelo, the difference between the 10% and 20% strain levels is significant with a p-value of 0.048. The same holds for the other strain levels of pomelo with the p-values between 0.023 and 0.013. The strain ratio values of citron simultaneously increase with increasing compression levels. The peels of lemon, grapefruit, and orange show no significant difference with increasing compression level. Compared to the samples of *Citrus* spp. the strain ratio of the PU foam samples markedly decreases with an

TABLE 5 Poisson's ratio (at 10% axial strain) and strain ratios (for >10% axial strain) at different strain levels for all tested citrus species: pomelo (*C. maxima*), citron (*C. medica*), lemon (*C.* x *limon*), grapefruit (*C.* x *paradisi*), orange (*C.* x *sinensis*), and for PU foam (RG35/50).

Species	*n*	Median Poisson's ratio and strain ratios at a specific axial strain level [median (IQR)]				
		10%	20%	30%	40%	50%
C. maxima	15	0.05 (0.05)	0.01 (0.05)	−0.02 (0.04)	−0.04 (0.04)	−0.03 (0.02)
C. medica	12	0.09 (0.18)	0.07 (0.06)	0.06 (0.06)	0.11 (0.04)	0.16 (0.06)
C. x *limon*	12	0.00 (0.29)	0.14 (0.07)	0.13 (0.10)	0.14 (0.05)	0.20 (0.10)
C. x *paradisi*	12	−0.08 (0.13)	−0.06 (0.06)	−0.05 (0.07)	−0.05 (0.05)	−0.09 (0.07)
C. x *sinensis*	12	−0.03 (0.14)	−0.03 (0.08)	−0.03 (0.03)	−0.05 (0.04)	−0.09 (0.02)
PU foam (RG35/50)	20	0.34 (0.25)	0.20 (0.07)	0.13 (0.04)	0.07 (0.04)	0.02 (0.05)

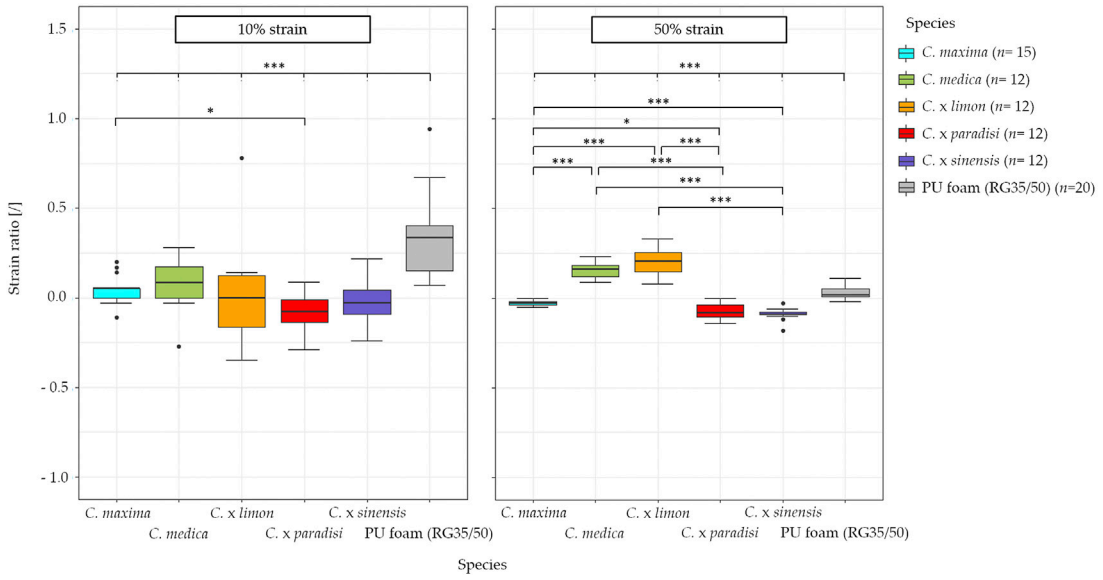

FIGURE 4
Comparison of the Poisson's ratio and the strain ratio for the tested *Citrus* species: pomelo (*C. maxima*), citron (*C. medica*), lemon (*C.* x *limon*), grapefruit (*C.* x *paradisi*), orange (*C.* x *sinensis*), and for PU foam at a strain level of 10% and 50% compression. The values are calculated with the manual image correlation method (MIC). All samples of *Citrus* spp. Are highest significant different from the ones of the PU foam (RG35/50).

increasing compression level. Remarkably, the differences in the individual compression levels of the peels of *Citrus* spp. are smaller in each case the difference to the PU foam. At the 10% strain level, all *Citrus* spp. samples show the highest interquartile range (IQR) in Poisson's ratio values compared to the strain ratios at higher compression levels (20%–50%).

The comparison of the Poisson's ratios of all fruit peels at a low level of compression (10%) shows that there exists a significant difference ($0.01 \leq p < 0.05$) between grapefruit and pomelo (Figure 4). More significant differences between the species are evident in the comparison of strain ratios at a compression of 50%. Thus, taken together we can see that at a compression of 50% lemon has the highest strain ratio (0.20), whereas grapefruit (−0.09) and orange (−0.09) have the lowest. In addition, the strain ratio of pomelo is slightly negative, while that of citron is slightly positive (Table 5).

The visual depiction of the characteristic deformation images (Figure 5-Figure 7, Supplementary Figure S2, S3, S4) illustrates that the outer lateral strain deformation is small throughout compression. Characteristic deformation images of pomelo (Figure 5), lemon (Figure 6) and PU foam (Figure 7) are presented below. Characteristic deformation images of citron, grapefruit, and orange can be found in the Supplementary Material (Supplementary Figure S2, S3, S4). The median strain

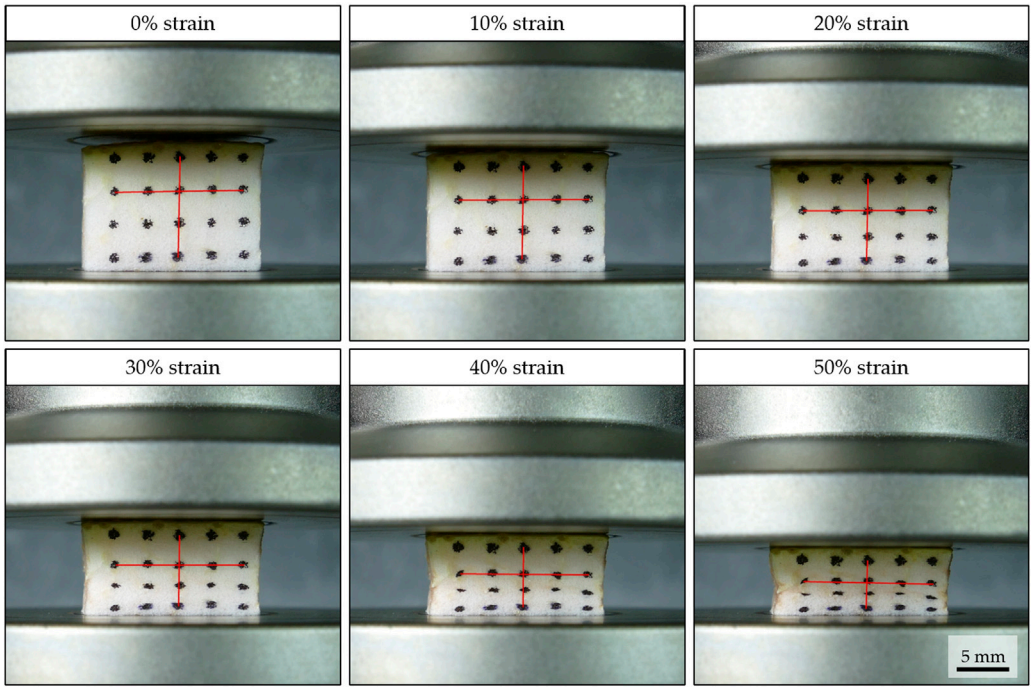

FIGURE 5
Characteristic deformation images of the peel of pomelo (*C. maxima*) at increasing strain. Sample height at a strain level of 0% equals 12.38 mm.

ratios of the pomelo are low and partly negative (Table 5). This is also reflected in the characteristic deformation images of pomelo (Figure 5). In the lateral direction, at an axial strain of 10%, barely any change can be detected. At an axial strain of 20% a deformation of the outer edges can be identified. In addition, especially in the middle of the sample (albedo region), the width of the sample is the smallest whereas the sample is the widest at the epidermis and endodermis region. This concave deformation increases with increasing strain levels. Furthermore, the distance between the second and third row of dots initially decreases most with increasing strain levels, resulting in a heterogeneous compression of the peel in the axial direction.

Compared to peels of the other tested *Citrus* species, the peel of lemon (*C.* x *limon*), which is significantly thinner than that of pomelo, shows the highest strain ratios for higher compression levels (Table 5; Figure 4, Supplementary Figure S1). The deformation images also show that the peel of lemon experiences a positive lateral deformation (Figure 6). More precisely, with an increasing compression level, the outer edges of the lemon peel show a convex deformation. Due to the low height of the specimen, only two rows of dots were able to fit. This limits the qualitative statement about the axial compression behavior. Nevertheless, it can be observed that the lower row of dots approaches the lower compression plate more closely and the upper row of dots comes more closely to the upper epidermis. Simultaneously, this indicates a heterogeneous deformation in the axial and lateral directions for this species.

The deformation images of the PU foam (RG35/50) barely reveal a change in the lateral direction at lower compression rates (Figure 7). Only at an axial compression of 30%, does a slight convex curvature of the outer edges become apparent, which then becomes more pronounced with increasing compression. Generally, the lateral compression is also very small in these specimens (Table 5). While a concave or convex curvature can be seen in all *Citrus* species, it is less distinctive in case of the PU foam samples. This indicates that the lateral deformation tends to be rather heterogeneous in the *Citrus* species. It is also noticeable that the sample behavior in the axial direction is contrary to that of pomelo. When comparing the images it becomes clear that when the rows of dots in the center of the pomelo sample are more compressed, whereas in the PU foam samples the upper and lower rows of dots are more compressed. (Figure 5-Figure 7).

3.3.2 Digital image correlation (DIC)

As mentioned before, Poisson's ratios describe the deformation behavior in the elastic range of a test specimen. The peels of *Citrus* spp. show no clear elastic range (Figure 3). Therefore, we chose a low axial strain level of 10% compression for the determination of the Poisson's ratio for all samples. Considering the Poisson's ratios of the samples, the values for the PU foam are significantly higher ($p < 0.001$) than the values of

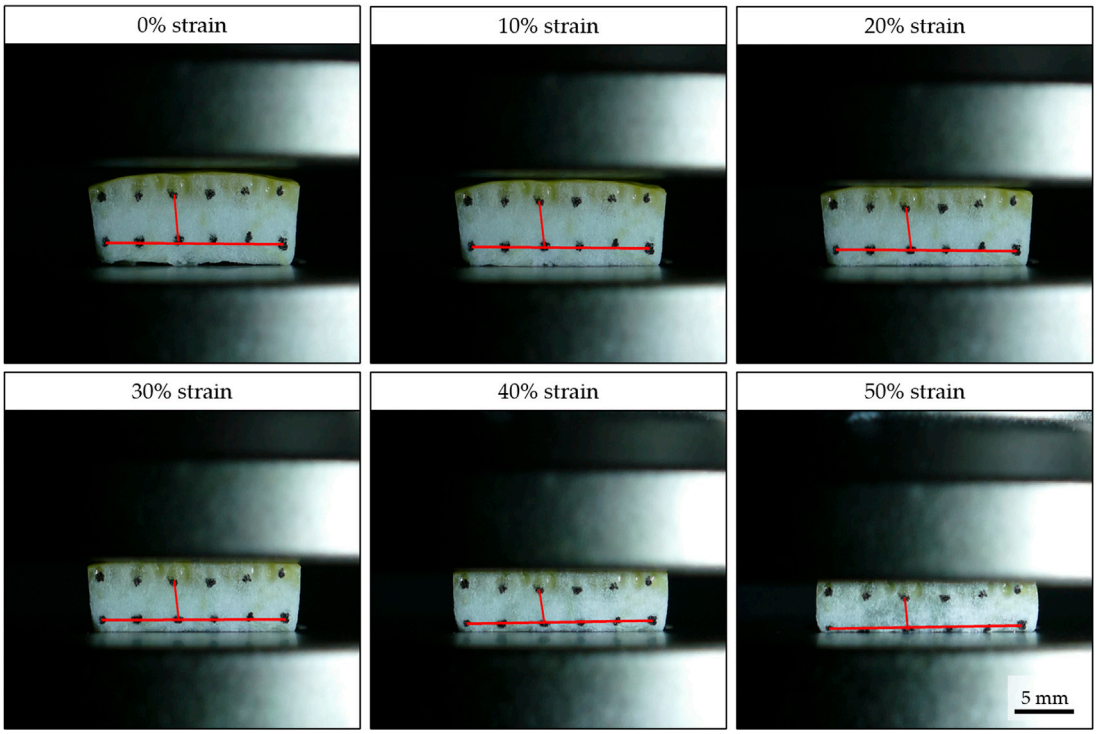

FIGURE 6
Characteristic deformation images of the peel of lemon (*C.* x *limon*) at increasing strain. Sample height at a strain level of 0% is 5.69 mm.

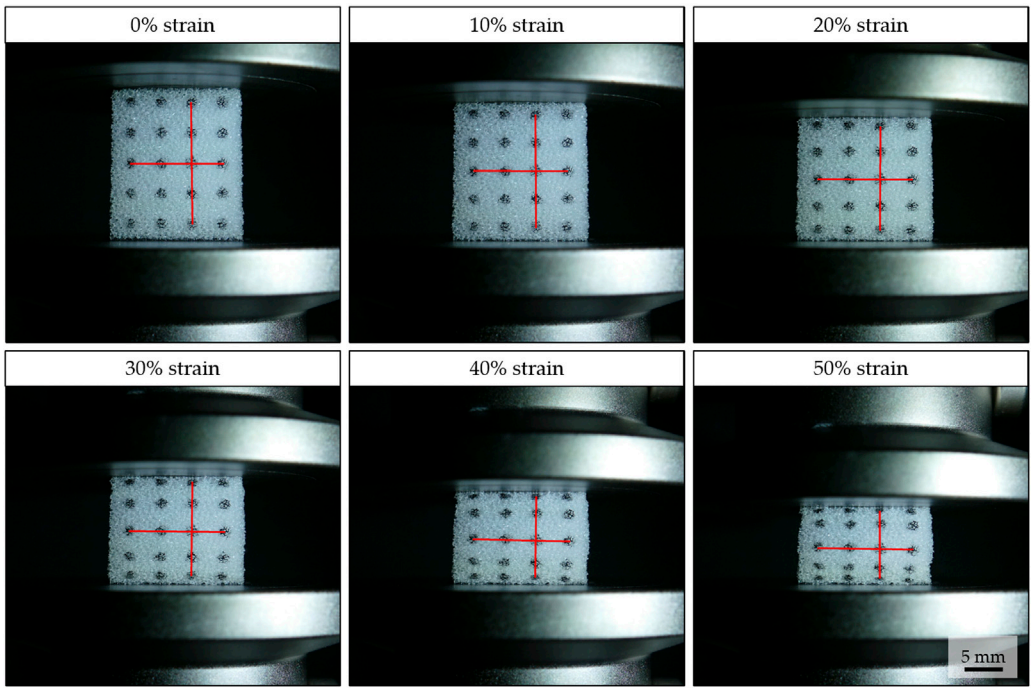

FIGURE 7
Characteristic deformation images of the PU foam (RG35/50) at increasing strain. Sample height at a strain level of 0% is 19.86 mm.

TABLE 6 Median Poisson's ratios at 10% axial strain for the tested citrus species: pomelo (*C. maxima*), citron (*C. medica*), lemon (*C.* x *limon*), grapefruit (*C.* x *paradisi*), orange (*C.* x *sinensis*), and for PU foam (RG35/50).

Species	*n*	Poisson's ratio (IQR)
C. maxima	14	0.00 (0.03)
C. medica	11	0.07 (0.06)
C. x *limon*	13	0.09 (0.14)
C. x *paradisi*	12	−0.02 (0.06)
C. x *sinensis*	12	−0.05 (0.07)
PU foam (RG35/50)	20	0.26 (0.12)

all citrus peel samples (Table 6), with the Poisson's ratios of the citrus peels being all close to 0. For example, orange shows the lowest Poisson's ratio with a median of −0.05, whereas lemon has the highest Poisson's ratio (0.09) among the citrus peels tested. The Poisson's ratios of lemon is thus significantly higher ($p < 0.001$) than that of orange and significantly higher ($0.01 \leq p < 0.05$) than that of pomelo and grapefruit, and the Poisson's ratio of citron peel is significantly higher ($p < 0.001$) than that of orange.

When comparing the results of the median Poisson's ratios determined by each method (DIC-method and MIC-method), no significant difference is apparent for any of the *Citrus* species and the PU foam tested (Figure 8). The MIC-method, however, shows more outliers and larger whiskers than the DIC-method.

The deformation of the specimens in the lateral direction up to an axial compression of 10% is visualized using the GOM Correlate 2019 software (Figure 9). The visualization shows that there exist always regions with negative lateral strain (>−5%) when compressing the peels of *Citrus* spp. (Figure 9, Supplementary Figure S5). The regions of negative strain are illustrated by the areas marked in red in Figure 9 and Supplementary Figure S5. The comparison shows that all species differ from each other in the arrangement of these regions. It should also be noted that the *Citrus* spp. samples also experience positive deformation in other regios of the sample (<5%, green marked area). The PU foam (RG35/50) shows solely positive deformations (<5%). The areas marked in red correspond to a compression of the area in lateral direction, whereas the green areas indicate an area expansion in lateral direction. The ratio and the amount of positive and negative deformation in lateral direction appear to be nearly equal. This militates for only a small general deformation in the lateral direction ($< \varepsilon_x$), which is simultaneously reflected in the low Poisson's ratios of *Citrus* spp. Only the tested PU foam samples (RG35/50) show larger Poisson's ratios and the visualization of the lateral strain clearly shows an increase in area, even if it is <5%.

4 Discussion

In this study, the compression behavior of a variety of citrus fruit peels was morphologically and mechanically characterized and compared with conventional polyurethane (PU) foam. The morphological comparison showed that the fruits of *Citrus* spp. not only differ in size and pulp color, but that the two largest fruits (pomelo and citron) have the significantly largest peel proportion. This in turn means they have the thickest peel but also have the lowest peel density compared to the other fruits tested (Section 3.1, Figure 2 and Table 3). On the one hand, these morphological characteristics could be attributed to the fact that pomelo and citron belong to the basic taxa (Nicolosi et al., 2000; Moore 2001). Therefore, they exhibit fewer cultivation artifacts compared to other fruits, which have been intensively crossbred as species and optimized, for example, to have a large amount of pulp (and consequently little peel), to allow for easy peeling, to show a specific color, to be seedless, and/or to have a high nutrition score (Stover et al., 2005; Abouzari and Mahdi, 2016). This kind of crossbreeding may be accompanied by a reduction or adaptation of other fruit tissues (Stover et al., 2005; Abouzari and Mahdi, 2016). On the other hand, a thicker peel with lower density is an obvious tool for damage protection. The peel protects the fruit and seed against damage from, for example, a drop from a tree or large shrub, thus ensuring attractiveness to vector animals that eat the fruit (Sharma et al., 2004), disperse the seeds, and thereby ensure species survival (Sharma et al., 2004; Bührig-Polaczek et al., 2016). This is especially relevant for the larger and heavier fruits, as they experience a high impact due to their own weight. In case of damage to the peel, microbes, bacteria or fungi could invade the fruit and rot it (Janzen 1977), meaning the seed would then not be dispersed by the vector animals.

Despite their morphological differences, all tested *Citrus* species show similar stress-strain characteristics. More specifically, the quasi-static compression tests with a relaxation phase up to an axial compression of 50% show that all tested peels of *Citrus* spp. exhibit a similar, slightly concave characteristic stress-strain curve, which differs only in the amount of stress (Figure 3; Table 4). All tested citrus peel samples show an increase in stress with increasing compression and a pronounced decrease in stress in the relaxation phase (Section 3.2). A clear linear-elastic range does not emerge in any of the fruit peels tested. This observation agrees with the results of Thielen et al. (2013a), who found neither a linear elastic range nor a plateau for the pomelo peel and partly contradicts the observation of Yang et al. (2022) and Wang et al. (2018) who characterized a linear elastic range for pomelo. Yang et al. (2022), however, also found no plateau, and calculated Poisson's ratios for axial strains up to 20% (Yang et al., 2022) or even up to 50% axial strain (Wang et al., 2018). Also in our study, no plateau regime as typical in synthetic foams [as in PU foam (Gong et al., 2005)] could be observed in *Citrus*

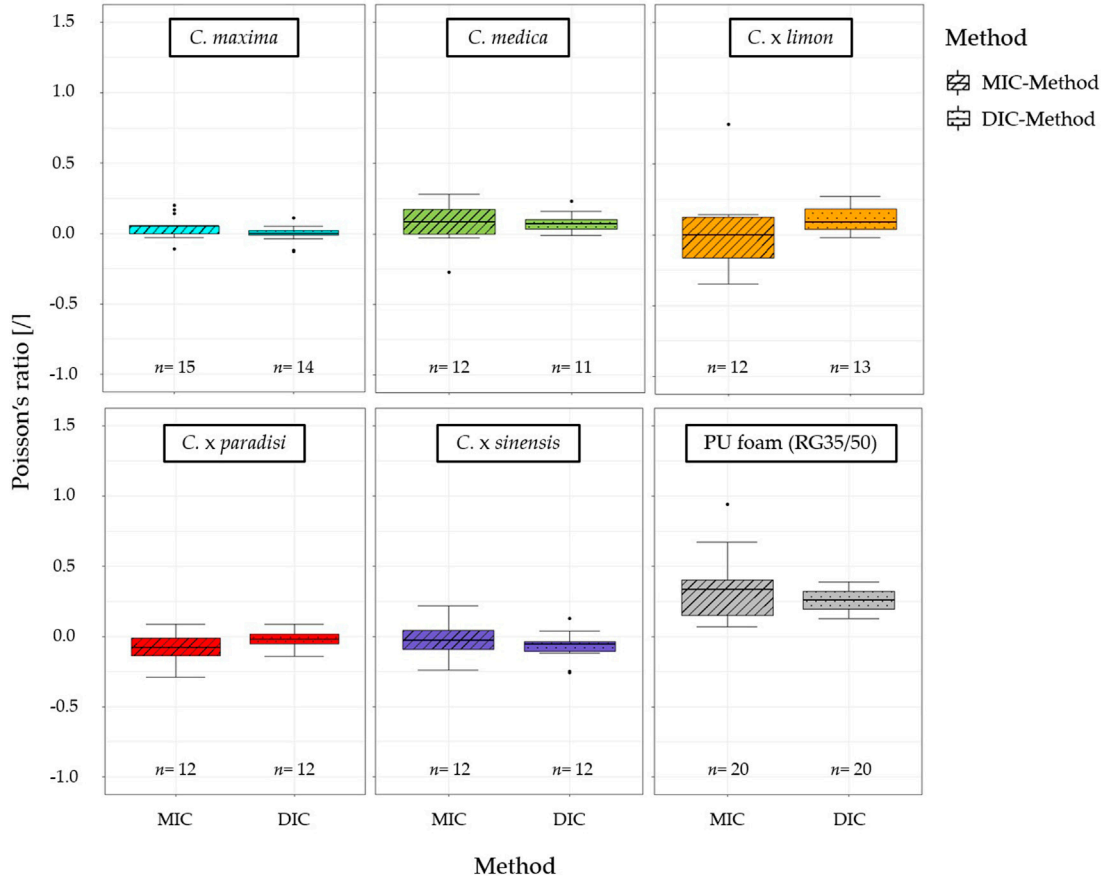

FIGURE 8
Comparison of the Poisson's ratios of the tested citrus species: pomelo (*C. maxima*), citron (*C. medica*), lemon (*C.* x *limon*), grapefruit (*C.* x *paradisi*), orange (*C.* x *sinensis*), and for the PU foam (RG35/50) calculated using the manual image correlation method (MIC) and the digital image correlation method (DIC). No significant differences between DIC and MIC occur for all tested specimens.

spp. (Gibson and Ashby, 1997), which was found for the tested PU foam (Section 3.2, Figure 3) (Li et al., 2006). The characteristic stress strain diagrams found for all tested *Citrus* species are more comparable to those of more compact tissues such as the fruit flesh of fresh apples (Oey et al., 2007). The characteristic stress-strain curve of the tested citrus peels is due to the fact that the compression of the fluid-filled cells (in flavedo) and the fluid-filled struts (in albedo) reduce the volume, which leads to a tautening of the cell walls (Thielen et al., 2013a). Once the cell walls are solidified, the deformation occurs at constant volume. This leads to stretching of the cell walls at higher stresses, compensating for volume reduction by compression or bending of the cells (Gibson et al., 2010). Relaxation is due to the viscoelasticity of the tissue and is a property of most biological materials (Niklas 1992). In the compression phases, the cells in the less dense areas of the peel (albedo) are the first to bend (Figure 5, Figure 6, Supplementary Figure S2, S3, S4). Once the specified strain is reached, the stress is released by further bending of the cells into the air-filled intercellular spaces (Thielen et al., 2013b). In addition, it can also be assumed that the yielding of the originally convex flavedo leads to a relaxation in the entire specimen. This effect however weakens with increasing compression, since the contact with the compression plate increases with each compression and relaxation interval (Thielen et al., 2013b). The viscoelastic behavior of the peels is extremely promising regarding damage prevention in bioinspired materials systems, as it results in a reduction of stress in the structure despite continuous compression, thus protecting the pulp and seed in the natural system.

Two analysis methods were used to characterize the compression behavior [MIC-Method (Section 3.3.1) and DIC-Method (Section 3.3.2)], as both have their advantages. The advantages of the MIC-Method are that it has a fast application and can operate at higher compression levels. Whereas the advantages of the DIC-Method are that is offers more reproducible, less fluctuating values at low compression levels. The software is able to track the significance over arbitrary positions in the sample. When looking at the Poisson's ratio and

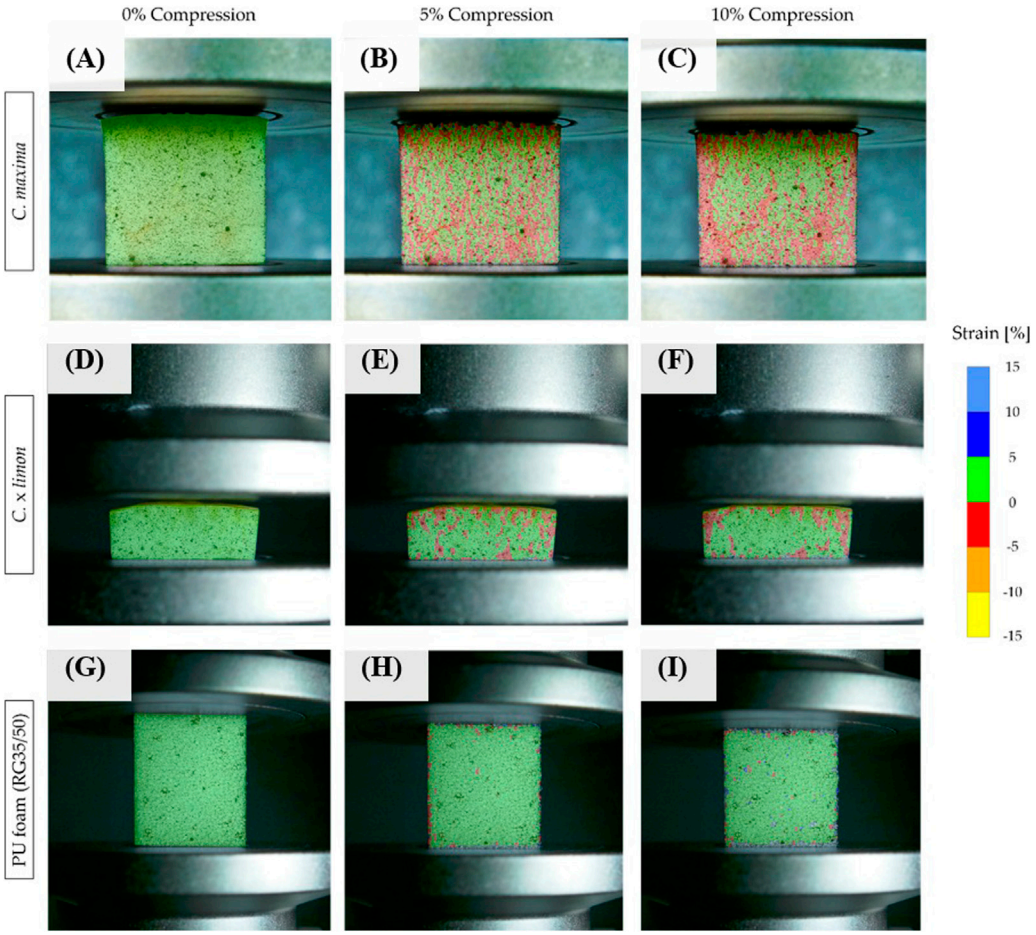

FIGURE 9
Visualization of the strain in lateral direction *via* GOM Correlate 2019 software. Characteristic deformation patterns up to an axial strain of 10% for **(A–C)** pomelo (*C. maxima*) **(D–F)** lemon (*C.* x *limon*), and **(G–I)** PU foam (RG35/50).

the strain ratio determined using the MIC-Method (Supplementary Figure S1), it is noticeable that up to a compression level of 20%, the peel samples of the tested *Citrus* species do not differ significantly from each other or only differ very slightly as in the case of pomelo ($p = 0.048$). This can be attributed to the fact that up to an axial compression of 20%, the very small deformations are affected by relatively strong fluctuations due to measurement inaccuracies, which has less effect on the measured values for larger deformations due to stronger axial compression. This is also reflected in the smaller whiskers, fewer outliers and the tendency towards smaller interquartile ranges at larger deformations (Table 5, Supplementary Figure S1). In addition to this, the "non-linear" behavior of the peel also matters for larger compressions because the Poisson's ratios are not constant. Thus, the Poisson's ratio for non-linear materials is often also expressed as a Poisson's function (Smith et al., 1999; Koumlis and Lamberson 2019). This Poisson's function corresponds to the tangent of the lateral-axial strain curve and describes the instantaneous value of the Poisson's ratio (Smith et al., 1999; Koumlis and Lamberson 2019). In this study, the Poisson's ratios were determined for low compressions, and the method used was also used to ensure comparability of the Poisson's ratios to the values determined by Wang et al. (2018) and Yang et al. (2022). In order to also determine the Poisson's ratio for higher compressions, one should consider calculating a Poisson's function as done by Koumlis and Lamberson (2019) according to Smith et al. (1999). While the strain ratio for pomelo decreases significantly with increasing axial compression, it increases significantly for citron. In contrast, the strain ratio for the three denser and thinner peels (lemon, grapefruit and orange) does not change significantly with increasing axial compression. The tested PU foam, on the other hand, shows a significant ($p < 0.001$) decrease in strain ratio with increasing axial compression. This leads to the conclusion that the thicker and less dense peel samples behave

more comparably to the foam, at least in their strain ratios. When comparing the MIC-derived Poisson's ratios of the different peel samples with each other (Figure 4A), it is noticeable that only pomelo and grapefruit differ significantly ($0.01 \leq p < 0.05$) from each other. In addition, all citrus peel samples are significantly different ($p < 0.001$) from PU foam (Figure 4A). At an axial compression of 50%, lemon has the highest strain ratio followed by citron and PU foam (Figure 4B). While the strain ratios of most citrus peel samples change only slightly with increasing strain level, the strain ratio of citron and lemon increases to the highest measured strain ratio (Table 5). Citron peel has a comparatively low density (532 kg/cm^3) and is rather thick (18.5 mm); whereas lemon peel shows a high density (784 kg/cm^3) and is rather thin (5.9 mm) (Section 3.1, Table 3). This disconnection between peel density and thickness shows that the increase in strain ratio is not exclusively due to the density or thickness of the peel, but that a combination of structural differences at the microscopic level influence the strain ratio especially at higher compressions. These differences in strain ratio between these two *Citrus* species are most likely due to graded changes in tissue density and cell turgescence, similar to the compaction behavior of pomelo (Thielen et al., 2013b). However, to substantiate this hypothesis one would need to analyze the individual structures of the different fruit peels on a submicroscopic ultrastructural and molecular level. This would be an essential step towards understanding in detail the structural differences of the different peels of *Citrus* spp. and thus towards drawing conclusions on the promising compression and damping behavior for further bioinspired applications.

Digital image correlation (DIC) was used to analyze the deformation of the *Citrus* species in more detail in the range of lower axial compression (≤10%) and to visualize the lateral deformation (Section 3.3.2). The Poisson's ratios of the peels of all five *Citrus* species studied, obtained by the DIC-Method, are close to zero (Table 6) and are not significantly different from those obtained by the MIC-Method (Figure 8). However, it should be taken into account that the values resulting from the DIC-Method are less scattered than the values obtained by the manual method (MIC), which is why the digital image correlation is more suitable for the determination of Poisson's ratios under low strain levels. It should also be noted that digital image correlation (DIC) has limited usage for compressions >20%. With increasing compression of the specimen, the stochastic pattern previously applied to the specimen disappears. In addition, the GOM Correlate software tracks fewer and fewer facets as the deformation increases, meaning that the evaluable range becomes less with increasing axial strain. This occurs especially in the area of albedo, which experienced the highest compression in most samples. The reduction of trackable facets with an increasing compression level can also be seen in Yang et al. (2022), who also used a digital image correlation software for a digital image analysis.

From the damage protection aspect, however, the low Poisson's ratios of *Citrus* spp. as well as the strain ratios at 50% axial compression, are particularly promising since these are all close to zero (with the exception of citron and lemon at higher strain levels). This means that there is not any, or only slight, expansion of the sample in the lateral direction during axial compression. Thus, the structure becomes denser and stiffer due to compression. Such dense and stiff structures can therefore better protect against damage impact than structures with higher Poisson's or strain ratios (Alderson 1999). The very low and partially negative lateral compression behavior is also reflected in the lateral edges of the deformation images (Figure 5). The pomelo shows a slightly concave form at the lateral edge of the test specimens and the other specimens show only an only slightly convex form (Figure 6, Supplementary Figure S2, S3, S4), but the lateral deformation is low in all cases even at compressions of 50%. This is also confirmed by the partly negative lateral strains visualized by the DIC-Method for all samples of *Citrus* spp. (Figure 9, Supplementary Figure S5). Although the pattern of partly negative lateral strain differs between the species and is moderate in amount (>−5%), it is sufficient to almost compensate for the positive lateral deformation that also occurs in the test samples. This means that overall there is very slight deformation in the lateral direction, resulting in very low, and in sometimes even slightly negative Poisson's ratios. The PU foam, on the other hand, does not show any negative lateral deformation, but also does not show any major positive lateral deformation, resulting in an overall larger median Poisson's ratio (0.26) compared to the tested citrus fruit peels.

Yang et al. (2022) also document a comparable compression behavior for the peel of pomelo at axial compressions of up to 70%. In addition, the Poisson's ratios determined by Yang et al. (2022) for the middle and lower albedo area are in the range of the Poisson's ratios determined by this study [0.00 (0.03)] for the entire pomelo peel. Only the values for the flavedo with a range of 0.239–0.346, determined by Yang et al. (2022), fall out of this range. The Poisson's ratios of Wang et al. (2018), which were determined using digital volume correlation, are also close to the Poisson's ratios determined in the present work for pomelo with a range of 0.08–0.11 ± 0.02 for axial compressions of up to 50%. This further supports the validity of the DIC-Method which was used in the present study. In addition, the low Poisson's ratios and the associated low lateral deformation behavior of the peels of the other tested *Citrus* species demonstrate that these can also serve as inspiration for technical damage protection and may be especially due to the sometimes low thickness of special interest.

5 Conclusion

This study showed that although the morphology of the peels differs (in thickness, density, Young's modulus and

maximum stress), all five tested citrus peels possess Poisson's ratios close to zero. A low or even negative Poisson's ratio is a key factor in terms of damage protection especially against impact. This is because a low Poisson's ratio in the *Citrus* spp. peel means it has a denser and more compact structure upon impact in the region of contact. When impacted the dissipative structure prevents damage because it has a low and partially negative lateral deformation. The viscoelastic properties of the peel are also noteworthy, as they lead to a reduction of stresses in the structure despite compression. In addition, this study highlights the respective advantages/disadvantages of both the manual image correlation (MIC) method and the digital image correlation (DIC). The MIC method proved to be quite effective in analyzing the compression behavior for higher strain levels (≥20%). Whereas DIC is preferable for evaluating and visualizing compression behavior for lower strain levels (<20%). Further investigation of the intercellular spaces and the density gradients of the different species on microscopic level is recommended. This would allow some conclusions on possible differences and similarities of the gradation of the structure and their influence on the damage protection of the structure.

Data availability statement

The raw data supporting the conclusions of this article are provided by the authors without reservation upon request.

Author contributions

TS supervised and initiated the study, and aquired the funding. MJ, MB, and FU carried out data collection, data assessment and the statistical analyses. Data evaluation and discussion of the results was a joint effort of all authors (MJ, MB, FU, TS). MJ wrote the first draft of the manuscript. All authors gave final approval for publication.

Funding

This research was funded by the Excellence Cluster livMatS [funded by the Deutsche Forschungsgemeinschaft (German Research Foundation, DFG) under Germany's Excellence Strategy–EXC-2193/1–390951807].

Acknowledgments

We acknowledge Michal Rössler for her artwork of the graphical abstract and Laura Mahoney for the language correction. The article processing charge was partly funded by the University of Freiburg in the funding program Open Access Publishing.

Conflict of interest

The authors declare that the research was conducted in the absence of any commercial or financial relationships that could be construed as a potential conflict of interest.

Publisher's note

Supplementary Material

The Supplementary Material for this article can be found online at: https://www.frontiersin.org/articles/10.3389/fmats.2022.979151/full#supplementary-material

References

Abouzari, A., and Mahdi, N. N. (2016). The investigation of citrus fruit quality. Popular characteristic and breeding. *Acta Univ. Agric. Silvic. Mendel. Brun.* 64, 725–740. doi:10.11118/actaun201664030725

Alderson, A. (1999). A triumph of lateral thought. *Chem. Industry* 17, 384–391.

Alderson, A., and Alderson, K. L. (2007). Auxetic materials. *Proc. Institution Mech. Eng. Part G J. Aerosp. Eng.* 221 (4), 565–575. doi:10.1243/09544100JAERO185

Allen, T., Martinello, N., Zampieri, D., Hewage, T., Senior, T., Foster, L., et al. (2015). Auxetic foams for sport safety applications. *Procedia Eng.* 112, 104–109. doi:10.1016/j.proeng.2015.07.183

Ashjari, M. (2017). Auxetic materials materials with negative Poisson's ratio. *MSEIJ* 1 (2). doi:10.15406/mseij.2017.01.00011

Bührig-Polaczek, A., Fleck, C., Speck, T., Schüler, P., Fischer, S. F., Caliaro, M., et al. (2016). Biomimetic cellular metals-using hierarchical structuring for energy absorption. *Bioinspir. Biomim.* 11 (4), 045002. doi:10.1088/1748-3190/11/4/045002)

Evans, K. E. (1991). Auxetic polymers: A new range of materials. *Endeavour* 15 (4), 170–174. doi:10.1016/0160-9327(91)90123-S

Fischer, S. F., Thielen, M., Loprang, R. R., Seidel, R., Fleck, C., Speck, T., et al. (2010). Pummelos as concept generators for biomimetically inspired low weight structures with excellent damping properties. *Adv. Eng. Mat.* 12 (12), B658–B663. doi:10.1002/adem.201080065

Ford, E. S. (1942). Anatomy and histology of the eureka lemon. *Bot. Gaz.* 104 (2), 288–305. doi:10.1086/335133

Gentile, A., La Malfa, S., and Deng, Z. (2020). *The citrus genome*. Cham: Springer International Publishing.

Gibson, L. J., Ashby, M. F., and Harley, B. A. (2010). *Cellular materials in nature and medicine*. Cambridge: Cambridge Univ. Press.

Gibson, L. J., and Ashby, M. F. (1997). *Cellular solids. Structure and properties*. Second edition. Cambridge, United Kingdom: Cambridge University Press Cambridge Solid State Science Series, 2.

Gong, L., Kyriakides, S., and Jang, W.-Y. (2005). Compressive response of open-cell foams. Part I: Morphology and elastic properties. *Int. J. Solids Struct.* 42 (5-6), 1355–1379. doi:10.1016/j.ijsolstr.2004.07.023

Janzen, D. H. (1977). Why fruits rot, seeds mold, and meat spoils. *Amercian Nat.* 111, 691–713. Artikel 980. doi:10.1086/283200

Jentzsch, M., Becker, S., Thielen, M., and Speck, T. (2022). Functional anatomy, impact behavior and energy dissipation of the peel of citrus × limon: A comparison of citrus × limon and citrus maxima. *Plants* 11 (7), 991. doi:10.3390/plants11070991

Klock, P., Klock, M., and Klock, T. A. (2007). *Das große ulmer-buch der Zitruspflanzen*. Stuttgart: Ulmer.

Koumlis, S., and Lamberson, L. (2019). Strain rate dependent compressive response of open cell polyurethane foam. *Exp. Mech.* 59 (7), 1087–1103. doi:10.1007/s11340-019-00521-3

Ladaniya, M. S. (2008). *Citrus fruit. Biology, technology and evaluation*. Amsterdam, Heidelberg, AmsterdamScienceDirect: Elsevier Academic Press.

Lakes, R. (1987). Foam structures with a negative Poisson's ratio. *Sci. (New York, N.Y.)* 235, 1038–1040. doi:10.1126/science.235.4792.1038

Li, Q. M., Magkiriadis, I., and Harrigan, J. J. (2006). Compressive strain at the onset of densification of cellular solids. *J. Cell. Plastics* 42 (5), 371–392. doi:10.1177/0021955X06063519

Li, T-T., Wang, H., Huang, S-Y., Lou, C-W., and Lin, J-H. (2019). Bioinspired foam composites resembling pomelo peel: Structural design and compressive, bursting and cushioning properties. *Compos. Part B Eng.* 172, 290–298. doi:10.1016/j.compositesb.2019.04.046

Moore, G. A. (2001). Oranges and lemons: Clues to the taxonomy of citrus from molecular markers. *Trends Genet.* 17 (9), 536–540. doi:10.1016/S0168-9525(01)02442-8

Nicolosi, E., Deng, Z. N., Gentile, A., La Malfa, S., Continella, G., and Tribulato, E. (2000). Citrus phylogeny and genetic origin of important species as investigated by molecular markers. *Theor. Appl. Genet.* 100 (8), 1155–1166. doi:10.1007/s001220051419

Niklas, K. J. (1992). *Plant biomechanics. An engineering approach to plant form and function*. Chicago, Ill: Univ. of Chicago Press.

Oey, M. L., Vanstreels, E., Baerdemaeker, J. D., Tijskens, E., Ramon, H., Hertog, M. L. A. T. M., et al. (2007). Effect of turgor on micromechanical and structural properties of apple tissue: A quantitative analysis. *Postharvest Biol. Technol.* 44 (3), 240–247. doi:10.1016/j.postharvbio.2006.12.015

R Core Team (2019). *R. A language and environment for statistical computing*. Vienna, Austria: R Foundation for Statistical Computing.

Ren, X., Das, R., Tran, P., Ngo, T. D., and Xie, Y. M. (2018). Auxetic metamaterials and structures: A review. *Smart Mat. Struct.* 27 (2), 023001. doi:10.1088/1361-665X/aaa61c)

Scott, F. M., and Baker, K. C. (1947). Anatomy of Washington navel orange rind in relation to water spot. *Bot. Gaz.* 108459 (4), 459–475. doi:10.1086/335434

Seidel, R., Thielen, M., Schmitt, C., Bührig-Polaczek, A., Fleck, C., and Speck, T. (2010). "Fruit walls and nut shells as an inspiration for the design of bio-inspired impact resistant hierarchically structured materials," in Proceeding of the DESIGN AND NATURE, 430. doi:10.2495/DN100371

Sharma, B. D., Hore, D. K., and Gupta, S. G. (2004). Genetic resources of Citrus of north-eastern India and their potential use. *Genet. Resour. Crop Evol.* 51 (4), 411–418. doi:10.1023/B:GRES.0000023456.70577.3d

Smith, C. W., Wootton, R. J., and Evans, K. E. (1999). Interpretation of experimental data for Poisson's ratio of highly nonlinear materials. *Exp. Mech.* 39 (4), 356–362. doi:10.1007/BF02329817

Speck, T., Bold, G., Masselter, T., Poppinga, S., and Schmier, S. (2018). "Biomechanics and functional morphology of plants - inspiration for biomechanic materials and structures," in *Anja Geitmann und Joseph Gril (Hg.): Plant Biomechanics* (ChamS: Springer International Publishing), 399–433.

Stover, E., Castle, W., and ChaoChih-Cheng, T. (2005). Trends in U.S. Sweet orange, grapefruit, and Mandarin-type cultivars. *horttech.* 15 (3), 501–506. doi:10.21273/HORTTECH.15.3.0501

Thielen, M., Speck, T., and Seidel, R. (2015). Impact behaviour of freeze-dried and fresh pomelo (citrus maxima) peel: Influence of the hydration state. *R. Soc. open Sci.* 2 (2), 140322. doi:10.1098/rsos.140322

Thielen, M., Speck, T., and Seidel, R. (2013b). Viscoelasticity and compaction behaviour of the foam-like pomelo (Citrus maxima) peel. *J. Mat. Sci.* 48 (9), 3469–3478. doi:10.1007/s10853-013-7137-8

Thielen, M., Schmitt, C. N. Z., Eckert, S., Speck, T., and Seidel, R. (2013a). Structure-function relationship of the foam-like pomelo peel (Citrus maxima)-an inspiration for the development of biomimetic damping materials with high energy dissipation. *Bioinspir. Biomim.* 8 (2), 025001. doi:10.1088/1748-3182/8/2/025001)

Ting, T. C. T., and Chen, T. (2005). Poisson's ratio for anisotropic elastic materials can have no bounds. *Q. J. Mech. Appl. Math.* 58 (1), 73–82. doi:10.1093/qjmamj/hbh021

Walther, A. (2020). "Viewpoint: From responsive to adaptive and interactive materials and materials systems: A roadmap," in Proceeding of the Advanced materials (Deerfield Beach, Fla.), e1905111. 32 20. doi:10.1002/adma.201905111

Wang, B., Pan, B., and Lubineau, G. (2018). Morphological evolution and internal strain mapping of pomelo peel using X-ray computed tomography and digital volume correlation. *Mater. Des.* 137, 305–315. doi:10.1016/j.matdes.2017.10.038

Widdle, R. D., Bajaj, A. K., and Davies, P. (2008). Measurement of the Poisson's ratio of flexible polyurethane foam and its influence on a uniaxial compression model. *Int. J. Eng. Sci.* 46 (1), 31–49. doi:10.1016/j.ijengsci.2007.09.002

Yang, B., Chen, W., Xin, R., Zhou, X., Tan, D., Ding, C., et al. (2022). Pomelo peel-inspired 3D-printed porous structure for efficient absorption of compressive strain energy. *J. Bionic Eng.* 19, 448–457. doi:10.1007/s42235-021-00145-1

Youssef, G., Kokash, Y., Uddin, K. Z., and Koohbor, B. (2022). Density-dependent impact resilience and auxeticity of elastomeric polyurea foams. *Adv. Eng. Mat.*, 2200578. doi:10.1002/adem.202200578